HOMO/LUMO Alignment at PTCDA/ZnPc and PTCDA/ClInPc Heterointerfaces Determined by Combined UPS and XPS Measurements

R. Schlaf and B. A. Parkinson

Department of Chemistry, Colorado State University, Ft. Collins, Colorado 80523

P. A. Lee, K. W. Nebesny, and N. R. Armstrong*,†

Department of Chemistry, University of Arizona, Tucson, Arizona 85721

Received: June 30, 1998; In Final Form: November 20, 1998

The offsets between the highest occupied molecular orbitals (HOMO) and the lowest unoccupied molecular orbitals (LUMO) at the 3,4,9,10-perylenetetracarboxylic dianhydride (PTCDA)/chloroindium phthalocyanine (ClInPc) and PTCDA/zinc phthalocyanine (ZnPc) organic heterojunctions were estimated from a combination of X-ray and ultraviolet photoemission (XPS,UPS) measurements. This combined method allows an improved determination of the electronic structure of such organic/organic′ interfaces due to the separate determination of the band bending (charge redistribution) following heterojunction formation. Both interfaces have large offsets in the onset for photoemission from their HOMO levels (PTCDA/ZnPc: 0.88 eV; PTCDA/CnlInPc: 0.93 eV). Using thin film absorbance data, the corresponding offsets in LUMO levels were estimated to be 0.66 eV (PTCDA/ZnPc) and 0.34 (PTCDA/ClInPc). The ZnPc/PTCDA interface showed a significant interface dipole (0.25 eV) while the ClInPc/PTCDA contact was essentially dipole free.

Introduction

Various perylenetetracarboxylic dianhydride dyes and phthalocyanines are promising materials for use as multilayer photovoltaics and photoconductor charge generation layers, transport materials, and lumophores in organic light emitting diodes (OLEDs) and as the channel region in organic thin film transistors.[1−3] Phthalocyanines generally demonstrate p-type conductivity, with reasonable hole mobilities,[1,4a] although appropriate heteroatom substitution in the Pc core, or addition of electron-withdrawing substituents (e.g. F, CN) can create n-type conductivity in these systems.[4b] In thin films of 3,4,9,10-perylenetetracarboxylic dianhydride (PTCDA) there have been some reports of p-type semiconductivity,[2e−h] other reports of impurity-dopant-based n-type conductivity,[1] and a recent report suggesting that both types of conductivity mechanism might hold, depending upon the orientation of molecular planes with respect to the measurement direction.[2a] The tetracarboxylic dianhydride bisimide derivatives of PTCDA generally have comparable HOMO and LUMO energies and have been shown to be primarily n-type conductors in pure thin films and photovoltaic heterojunctions[1,5a,c]). Heterojunctions based on thin films of PTCDA or its related bisimides, and certain phthalocyanines, show a marked tendency toward exciton dissociation at the Pc/PTCDA interface[1b,c,f,2c,5,6]

These exciton dissociation processes are presumed to be assisted by the presence of fixed charges or high dipolar fields, as a result of charge transfer processes across the heterointerface.[6] It is therefore of considerable interest to determine the alignment between the highest occupied molecular orbitals (HOMO) and the lowest unoccupied molecular orbitals (LUMO) of both components of the O/O′ heterojunction at these

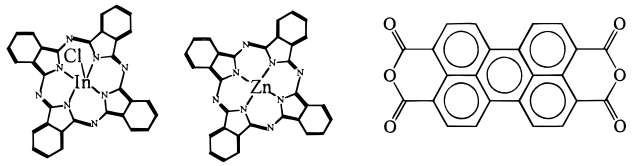

ClInPc ZnPc PTCDA

interfaces, as a means of assessing the relative donor and acceptor properties of these materials in the condensed phase.

Previous attempts to determine the relative HOMO energies of dissimilar organic thin films using photoelectron spectroscopies have taken several different approaches, including (a) deposition as ultrathin films on metals such as gold, using the underlying Fermi level of the substrate as the common energy reference level,[5a−c] (b) characterization of ultrathin films on these same metals, correcting for work function changes which occur during deposition of the thin films, and then assumption of a common vacuum level,[5e] and (c) direct measurement of shifts of the effective work function of the metal substrate/organic thin film system, thereby not assuming a common vacuum level for either the substrate or any thin film deposited over it.[2d,5f−h] All of these methods appear to allow for a self-consistent estimation of the differences in HOMO levels of dissimilar organic materials, but produce significant differences in estimation of the barrier heights for hole or electron injection between conductors and organic layers and may not provide for a complete description of the charge redistribution which occurs in these thin films up to several molecular layers away from the critical heterojunction interface.

Our recent studies of heterojunctions based upon layered inorganic semiconductor materials, such as $MoSe_2$ thin films grown on SnS_2 substrates (where the interactions between the layer planes are weak, as in molecular solids), suggest that a *combination* of UV and X-ray photoemission spectroscopies

* To whom correspondence should be addressed.
† E-mail: nra@u.arizona.edu.

10.1021/jp982834y CCC: $18.00
Published on Web 03/26/1999

(UPS and XPS) is needed to fully characterize both the interfaces between conductors and organic thin films, and organic/organic′ interfaces, and that common vacuum levels should not be assumed when such interfaces are created.[7,8] For various inorganic semiconductor heterojunctions, composed of two different materials A and B, a simultaneous combination of UPS and XPS measurements has been carried out during a multistep growth sequence of a thin film of semiconductor B on a substrate of semiconductor A.[7−10] We have recently shown that this method can also be applied effectively to the characterization of the HOMO offsets of organic semiconductor heterojunctions used in electroluminescent devices,[11a] and Shimada et al. have recently applied the same approach to the characterization of heterojunctions based upon copper phthalocyanine and various layered inorganic semiconductors, with widely variable work functions (4.0−5.5 eV) and otherwise weak, van der Waals-like interactions with the organic overlayer.[11b]

The goal of such measurements is the determination of HOMO and LUMO alignment at the interface between two layers of materials A and B, thick enough to possess "bulk electronic structure". For this reason only the HOMO position of a relatively thick layer of B should be compared with the HOMO position of the clean substrate layer A. In thin layers one faces the possibility that the HOMO line shape and position have not yet reached the final bulk condition, since the interactions between dissimilar molecules, involving dispersion forces, dipolar interactions and partial charge transfer, may take several molecular layers to fully develop. Another problem with the evaluation of photoemission spectra from thin overlayers is the superposition of photoelectron emissions from the substrate layer and overlayer, which affects the measurement accuracy, due to the necessity of using fitting procedures to determine the HOMO positions of both materials separately. To circumvent these problems the second component (B) of the heterojunction needs to be grown to thicknesses which allow it to exhibit a bulklike line shape and possess a thickness which exceeds the sampling depth of the photoelectrons in UPS measurements of component A (e.g. 3× the inelastic mean free path of the photoelectrons, 5−20 Å[12]). The problem with this approach is that, at the relatively high layer B thicknesses required, significant amounts of charge redistribution (band bending) can develop in both the substrate and overlayer, which shift the HOMO positions on an absolute energy scale. These phenomena are observable in the formation of semiconductor heterojunctions based upon three-dimensional materials, weakly interacting layered inorganic semiconductors, and molecular solids. With XPS this band bending can be measured directly by monitoring the shifts of representative, energetically well resolved, XPS core level peaks of substrate and overlayer, during the growth process.[7,8] It may also be important that a growth mode close to layer-by-layer growth in both components of the heterojunction be achieved (see below).

We will demonstrate here the application of this approach to the characterization of PTCDA/ClInPc and PTCDA/ZnPc bilayers, where measurable amounts of band bending develop during formation of the heterojunction. The trivalent metal Pcs (ClAlPc, ClGaPc, and ClInPc) and the related tetravalent metal Pcs (VOPc and TiOPc) can exhibit layered growth as thin films,[13] as can both PTCDA and C4-PTCDI.[14] These are therefore good candidates for the formation of O/O′ heterojunctions. ZnPc is representative of the divalent metal Pcs, and while not normally demonstrating layered growth, has a precontact HOMO position sufficiently different from the trivalent and tetravalent metal Pcs as to make it useful in comparing the energetic nature of the first few molecular layers of Pc/PTCDA heterojunctions.

Experimental Section

The experiments were carried out in a VG ESCALAB MkII UHV spectrometer equipped with XPS, UPS, and a connected growth chamber, allowing *in situ* characterization of the prepared films (base pressure 10^{-9} mbar). The organic dyes were obtained from Aldrich and entrainer-sublimed to achieve adequate purity before use. The central cut (ca. 20%) of the pure fraction in the entrainer was collected for each purification step, and if necessary, a second entrainer sublimation process was used to obtain a pure dye fraction. The organic compounds were evaporated from BN-crucible-equipped Knudsen cells, which were maintained at temperatures just below the growth temperature during the pump-down cycle of the growth chamber. The growth rate for all layers was about 2−3 Å/min as was determined by a quartz thickness monitor positioned near the samples. The substrates were at ambient temperature (20 °C) during growth. The organic heterojunctions were prepared by first growing a 256 Å film of 3,4,9,10-perylenetetracarboxylic dianhydride (PTCDA) on the basal planes of SnS_2 crystals which were cleaved *in vacuuo* immediately before film growth. SnS_2 was used because of the chemical inertness of its basal plane and its easy cleavability due to its two-dimensional crystal structure,[15−17] and because PTCDA can exhibit layered growth on SnS_2.[13,14b] PTCDA also grows epitaxially on highly oriented pyrolytic graphite (HOPG) and MoS_2 which have similar surface structures to SnS_2.[18−20] Chloroindium phthalocyanine (ClInPc) and zinc phthalocyanine (ZnPc) layers were grown in several steps on the PTCDA film. After each growth cycle the samples were characterized by XPS and UPS to determine the highest occupied molecular orbital (HOMO) alignment. The XPS characterization of the samples after each growth step was performed with Mg Kα radiation at 50 eV pass energy. The spectrometer was calibrated to yield 75.13 eV for the Cu(3p) doublet and 932.66 eV for the Cu($2p_{3/2}$) line positions, on an atomically clean Cu substrate. Very small shifts in binding energy are observed accompanying the charge redistribution process which parallels formation of these heterojunctions. The reproducibility in determining these energies was ±0.01 eV, determined by occasional recalibration of the spectrometer with the clean Cu surface. All given XPS line positions and fwhms were determined by a fitting procedure described in ref 20. UPS was performed with −5 V bias voltage applied to the sample using the He(I) (21.21 eV) line, at a 5 eV pass energy not corrected in the UPS data below.

Results and Discussion

Evaluation of Photoemission Spectroscopy (PES) Data. The combination of UPS and XPS measurements allows the direct determination of the HOMO offset ΔHOMO, the interface dipole eD, and an indication of the charge redistribution or band bending, V_b, across the interfacial region. By including the optical gaps, E_g, of the materials determined from absorption measurements in thin films an *estimate* of the LUMO offset (ΔLUMO) can also be determined. Depending upon the exciton binding energy (which for some organics can be as high as 1.0 eV), aggregation effects, etc., it is recognized that the true LUMO position, responsible for electronic conduction in the solid, will not likely be at the LUMO position estimated from these optical measurements.[21] Nevertheless, these measurements are useful as a way of providing a semiquantitative indication of the offsets anticipated in LUMO levels at these heterojunctions.

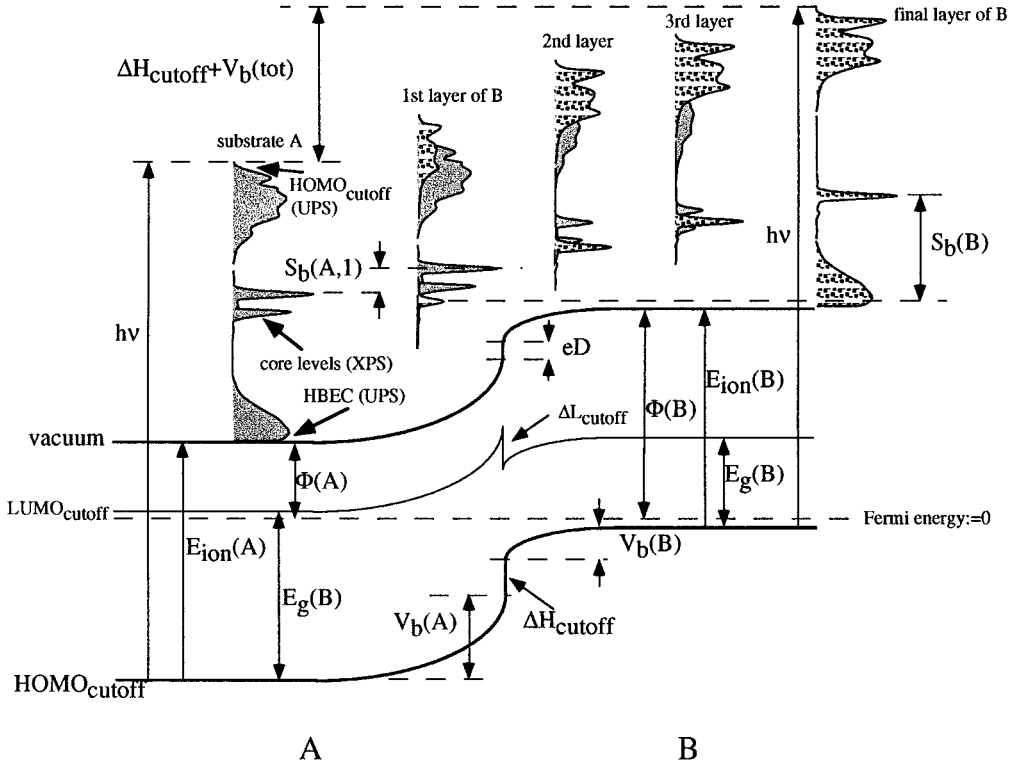

Figure 1. Schematic of the HOMO/LUMO alignment at organic semiconductor heterointerfaces and the resultant XPS and UPS photoemission. The lower part of this figure shows the electronic structure of a typical interface composed of two compounds A and B which have different ionization energies E_{ion}, work functions Φ, optical gaps E_g, and Fermi energies. The top part shows schematic photoemission spectra as they develop during the multistep growth procedure. The offset between the HOMO cutoffs on both sides, ΔH_{cutoff}, is determined from UP spectra by measuring the binding energy of the cutoff of the uncovered substrate and then after completion of the final layer. The difference between these values equals the sum of the total band bending $V_b(tot)$ across the structure plus ΔH_{cutoff}. Therefore, $V_b(tot)$ is measured separately by monitoring the shifts of the core level spectra measured with XPS.

Figure 1 shows a schematic of the frontier orbital energies for heterojunction components A and B, as layers of B are added. This schematic is drawn from the assumption that the initial component of the heterojunction (A) has a larger energy gap than component B, as in the organic systems discussed here, and that the HOMO for A is farther from the vacuum level than the HOMO for B, which are typical conditions for the studies discussed here. The bottom part of this figure shows an assumed electronic structure at the heterointerface A/B, with the assumption that charge redistribution or band bending occurs over a few molecular layers. On the top part of this figure the evolution of the PE spectra during the growth process is shown. From the left to the right schematic spectra for the uncovered substrate ("substrate A") and spectra obtained after growth of the first to final layers of material B are displayed.

The spectra in Figure 1 are shown for simplicity as though only one exciting light source is used. In the measurements presented here, however, the positions of the HOMO cutoff ($HOMO_{cutoff}$) and the high binding energy cutoff (HBEC) were determined from He(I) UP spectra, while the core levels were measured with XPS (Mg Kα radiation), which therefore produce spectral peaks from photoemission events with widely varying kinetic energies. The core level spectra in Figure 1 are portrayed for simplicity as having kinetic energies which would make them appear in the middle of the UPS spectral region.

From the low binding energy cutoff of the UP spectra the change in absolute energy of the HOMO cutoff is determined. To show the changing contributions of A and B to the VB spectra the photoemissions from substrate and overlayer are shown separated in Figure 1. The real spectra, however, are typically a superposition of both. The HBEC of the UP spectrum allows estimation of the position of the vacuum level relative to the Fermi level. For each deposition, equilibration of layers A and B with the conductive SnS_2 substrate and the spectrometer, is assumed. Therefore, subtracting HBEC from the excitation energy ($E = h\nu = 21.2$ eV) directly yields the effective work function Φ.[22] The ionization energy E_{ion} is determined by adding the $HOMO_{cutoff}$ to Φ. By following the unique shifts of the XPS core levels of substrate and overlayer, any additional band bending across the interface can be determined.

The HOMO/LUMO alignment at the interface is then determined as follows: First, the total shift, ΔHOMO, of the HOMO cutoff energy is determined from clean substrate A to completed overlayer B by computing the difference in their cutoff energies. As is evident from Figure 1, ΔHOMO consists of the HOMO offset, ΔH_{cutoff}, plus the combined energy shift due to band bending or charge redistribution $V_b(tot) = V_b(A) + V_b(B)$ in A and B. $V_b(tot)$ is typically determined by adding the shift of the core level XPS peak for substrate A, after growth of the first layer of B on A ($S_b(A,first)$), to the total shift of the core level XPS peak for B from this first layer to the final layer ($S_b(B)$). $S_b(B)$ contains both substrate and overlayer band bending developing after the first layer of B is grown:

$$V_b(tot) = S_b(A,first) + S_b(B) \quad (1)$$

With this value we determine ΔH_{cutoff} according to

$$\Delta H_{cutoff} = \Delta HOMO - V_b(tot) \quad (2)$$

The corresponding offset between the LUMOs of A and B is then estimated (see above) by inserting the optical gaps E_g of

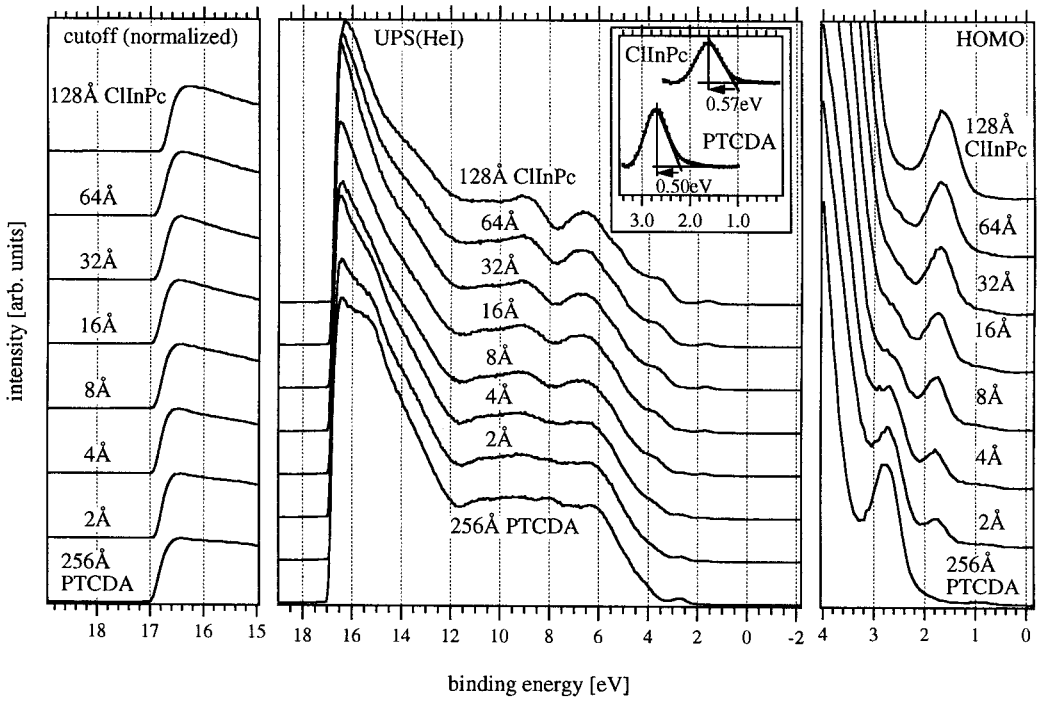

Figure 2. UPS data for the bare 256 Å PTCDA film and this same surface after each growth step of the ClInPc overlayer. In the right panel the HOMO spectra are shown magnified for more detail. The HOMO of the PTCDA layer at about 2.8 eV is successively attenuated by the increasing thickness of the ZnPc layer whose HOMO arises at about 1.8 eV. In the left panel the high binding energy cutoff is shown normalized to allow for easier visualization of the shifts in energy. The insert in the center part shows the background removed HOMO peaks of the uncovered substrate and the final ClInPc overlayer. The line fit and maxima positions which were used for the determination of the HOMO cutoff to maximum (HCM) energy for both compounds are included into the graph.

both materials into

$$\Delta L_{\text{cutoff}} = \Delta H_{\text{cutoff}} - [E_g(\text{B}) - E_g(\text{A})] \qquad (3)$$

In the phthalocyanines there can be substantial variation in the optical gap energy, estimated from an absorbance spectrum of a thin film. Aggregation effects can move the absorbance maxima over a range of ca. 630−830 nm, depending upon the packing patterns between adjacent Pc rings.[21] In these studies we have used the absorbance maximum for epitaxially grown ClInPc thin films on PTCDA ($\lambda_{\text{max}} = 760$ nm, optical gap = ca. 1.6 eV) and for β-phase ZnPc films (no demonstration of epitaxy) grown on a variety of substrates where islandlike growth occurred ($\lambda_{\text{max}} = 630$ nm, optical gap = 2.0 eV). As discussed above, these optical gaps can only be lower limit estimates to the true band gap of these solids, but nevertheless provide a useful means of approximating the changes likely to occur to their energies at the heterojunction interface.

From Figure 1 it is evident that the interface dipole eD contribution to UPS and XPS peak shifts can be calculated by subtracting V_b(tot) from the difference of the substrate and final layer work functions. This is equivalent to calculating

$$\text{eD} = \Delta H_{\text{cutoff}} - [E_{\text{ion}}(\text{B}) - E_{\text{ion}}(\text{A})] \qquad (4)$$

This interface dipole, eD, therefore corresponds to the deviation of the measured HOMO offset ΔH_{cutoff} from the value expected by the electron affinity rule (EAR)[7,23] which assumes alignment at the vacuum level. Seki and co-workers have recently demonstrated this type of interface dipole formation at the interface between two dissimilar donor−acceptor-complex-forming organic species.[5g,h]

In the data evaluation below we use the following conventions: heterojunctions are evaluated from the substrate on the left to the overlayer on the right as in Figure 1. Coming from the left in Figure 1, energy shifts, energy offsets, and dipolar field contributions toward higher binding energy (pointing down in Figure 1) are positive, while shifts to lower binding energy are negative. E_g, Φ, and E_{ion} are always positive. Fermi energy is zero energy.

Determination of the Electronic Structure of the Interfaces. *The PTCDA/ClInPc Heterojunction*. The UP spectra taken after each Pc growth step are shown in Figure 2. The center part of this figure shows the complete spectra. The right-hand panel shows the HOMO emission regions in more detail, while the left-hand panel shows the high binding energy cutoff (HBEC) with normalized intensity to allow better comparison between spectra. The bottom spectrum in each series corresponds to the initially deposited, 256 Å thick PTCDA layer, which served as substrate for the formation of the heterojunction. With increasing ClInPc coverage the PTCDA spectra give way to the more distinct photoemission peaks of the ClInPc overlayer. In the HOMO emission region the PTCDA HOMO peak steadily vanishes while the ClInPc HOMO increases in intensity at lower binding energy. The HBEC position shifts to lower binding energy at higher ClInPc coverages, corresponding to an increase of the effective work function of this heterojunction. The insert in the center part shows the HOMOs of the uncovered substrate and the final layer with the secondary emission background removed by fitting the integrated intensity curve into the kinetic energy region below the peaks.[7,8,11] The remaining spectra were fit by Gaussian−Lorentzian combination peaks to determine the maximum positions. Also shown are the fitted line shapes used to determine the HOMO cutoff energy. This yields a HOMO cutoff to maximum (HCM) distance of 0.50 eV for PTCDA and 0.57 eV for ClInPc.

Figure 3 shows XP core level spectra of the PTCDA substrate and ClInPc overlayer. The O(1s) spectra in the PTCDA layer shown at the bottom decrease in intensity with increasing ClInPc

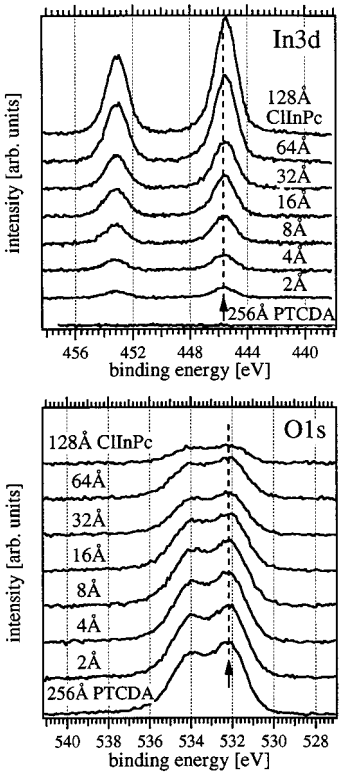

Figure 3. XPS data of the O(1s) and In(3d) core levels as a function of ClInPc coverage over the PTCDA substrate layer.

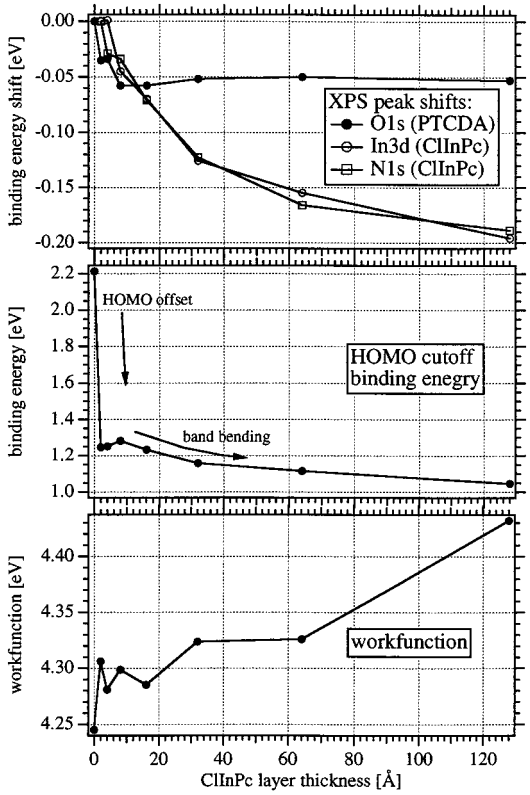

Figure 4. XPS line shifts (top), HOMO cutoff binding energy (center), and work function (bottom) depending on the ClInPc layer thickness. The development of band bending is evident from the XPS line shifts.

coverage. The O(1s) emission X-ray peaks reflects the different chemical state of the two oxygen forms in the dianhydride portion of this molecule.[24] The spectra show a slight shift (−0.05 eV) to lower BE with increasing ClInPc coverage. The intensity of the In(3d) spectra of the ClInPc layer, shown in the top graph, increases systematically with the film thickness. A larger shift in In(3d) peak energies versus those seen for the O(1s) peak is observed as a function of Pc coverage, which relates mainly to larger amounts of band bending or charge redistribution developing in the ClInPc film.

The shifts of both photoemission lines, plus shifts of the ClInPc related N(1s) line (spectra not shown) are shown versus apparent Pc layer thickness in Figure 4a. In the center part (Figure 4b) the shift of the HOMO cutoff vs layer thickness is shown. The large shift between the first two points represents the transition observed with the first layers of ClInPc on PTCDA, while the smaller shifts at higher coverages are related to the further development of band bending or charge redistribution in this interfacial region. The bottom graph (Figure 4c) shows the development of the effective work function Φ with increasing layer thickness. Even though we show this plot on an expanded scale, the total shift in Φ is only twice the uncertainty in our measurements, and is small compared with systems which demonstrate a measurable interface dipole (see below).

The band bending across the entire interface can now be estimated using eq 1. The charge redistribution shift observed in the PTCDA O(1s) line, after growing the first ClInPc layer, amounts to S_b(PTCDA,first) = −0.04 eV. The total shift of the In3d and N(1s) lines is represented by S_b(ClInPc) = −0.20 eV. This leaves

$$V_b(\text{tot}) = S_b(\text{PTCDA,first}) + S_b(\text{ClInPc}) = -0.23\ \text{eV}$$

Since the O(1s) peak is still visible at the final Pc layer thickness it is possible to determine the amounts of band bending present on both sides separately. The total shift of the O(1s) line of −0.05 eV equals the band bending in the PTCDA layer:

$$V_b(\text{PTCDA}) = -0.053\ \text{eV}$$

The band bending in the ClInPc layer is determined by calculating

$$V_b(\text{ClInPc}) = V_b(\text{tot}) - V_b(\text{PTCDA}) = -0.18\ \text{eV}$$

In order to determine the HOMO cutoff offset ΔH_{cutoff} using eq 2, the HOMO cutoff shift between uncovered PTCDA substrate and final ClInPc layer, ΔHOMO, needs to be determined. The spectral line fits into the background-corrected HOMO peaks yield 2.21 eV for the PTCDA HOMO cutoff and 1.05 eV for the ClInPc HOMO cutoff of the final layer. Therefore, ΔHOMO amounts to −1.16 eV. It follows that

$$\Delta H_{\text{cutoff}} = \Delta\text{HOMO} - V_b(\text{tot}) - 1.16\ \text{eV} - (-0.23) = -0.93\ \text{eV}$$

Using the HCM values for PTCDA and ClInPc determined above, the offsets between the HOMO maxima are estimated:

$$\Delta H_{\text{max}} = \Delta H_{\text{cutoff}} + [\text{HCM(ClInPc)} - \text{HCM(PTCDA)}]$$

$$\Delta H_{\text{max}} = -0.93\ \text{eV} + [0.57\ \text{eV} - 0.50\ \text{eV}] = -0.86\ \text{eV}$$

Inserting the presumed optical gaps of both materials (E_g(PTCDA) = 2.22 eV,[27] E_g(ClInPc) = 1.63 eV[21]) into eq 3 yields

$$\Delta L_{\text{cutoff}} = -0.93 - [1.63\ \text{eV} - 2.22\ \text{eV}] = -0.34\ \text{eV}$$

for the offset between the LUMO cutoffs.

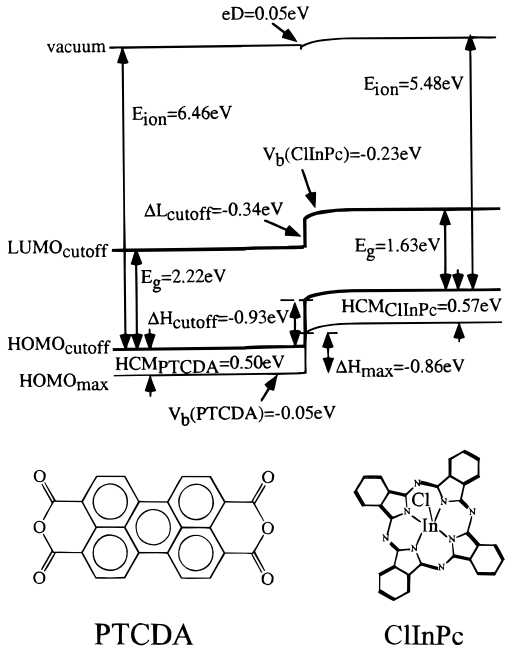

Figure 5. Summary of the evaluation of the HOMO/LUMO alignment at the PTCDA/ClInPc heterointerface. The HOMO offset between PTCDA and ClInPc was determined to −0.93 eV (cutoff) and −0.86 eV (maxima). From known values for the HOMO−LUMO gaps the cutoff offset of the LUMO was determined to be −0.34 eV. A weak interface dipole of 0.05 eV is present at the interface.

The remaining parameter to determine is the interface dipole eD. The ionization energies E_{ion} of PTCDA and ClInPc are obtained by adding work functions and HOMO cutoff positions of the clean substrate and final ClInPc layer spectra:

$$E_{ion}(\text{PTCDA}) = 4.25\ \text{eV} + 2.21\ \text{eV} = 6.46\ \text{eV}$$

$$E_{ion}(\text{ClInPc}) = 4.43\ \text{eV} + 1.05\ \text{eV} = 5.48\ \text{eV}$$

Including these values into eq 4 together with ΔH_{cutoff} yields eD = −0.93 eV − [5.48 eV − 6.46 eV] = 0.05 eV which is a nearly negligible interface dipole effect. The results of these estimations describing the energetics of the PTCDA/ClInPc heterojunction are summarized in Figure 5.

The PTCDA/ZnPc Heterojunction. Figure 6 shows the UP spectra on the uncovered PTCDA substrate and after each ZnPc growth step. Figure 7 shows the key core level XPS data obtained for both layers at the same coverages. Figure 8 summarizes the relevant energy shifts obtained from both UPS and XPS data. With increasing ZnPc coverage the PTCDA spectral features vanish while the distinct peaks of ZnPc arise. Figure 7 shows that during the first growth steps of ZnPc on PTCDA a significant shift of almost 0.5 eV occurs in the HBEC, which mainly arises due to the presence of an interface dipole (see below). The development of the effective work function vs film thickness, as determined from the HBEC positions, is shown in the bottom graph of Figure 8.

On the right side of Figure 6 the HOMO spectral range is shown in more detail. Similar to the PTCDA/ClInPc interface, photoemission from the HOMO of the PTCDA film is gradually replaced by that from the HOMO of the ZnPc layer. The shift to higher binding energy of the PTCDA HOMO is related to the development of charge redistribution in the PTCDA layer. The insert in the center part of this figure shows the HOMO cutoff to maximum distances for both pure components are determined. The base width for the PTCDA HOMO peak is 0.50 eV, which reproduces the value measured in the PTCDA/ClInPc junction. The HCM of ZnPc, HCM(ZnPc) = 0.43 eV, is smaller than the value determined for ClInPc. The change of HOMO cutoff position with increasing coverage is presented in Figure 8b. The 0.18 eV increase of its binding energy is related to the development of band bending in the PTCDA layer. The data points at larger Pc coverages were taken from the developing ZnPC HOMO, which led to the large step toward lower binding energy. This step mainly corresponds to the offset between the PTCDA and ZnPc HOMO. The following weak backshift to higher binding energy corresponds in part to the further development of band bending, as well as to a slight change in the HOMO shape with increasing Pc film thickness.

The development of band bending in the substrate PTCDA film with increasing ZnPc coverage is evident from the slight shift to higher binding energy of the O(1s) line (Figure 7) while it is attenuated by the growing thickness of the ZnPc layer. In contrast to that, the intensity of the Zn(2p) line increases with ZnPc coverage, while no significant binding energy shifts are detected. The shifts of both lines are plotted vs effective ZnPc thickness in Figure 8a. From this graph we determine the band bending across the interface. The total shift of the O(1s) peak amounts to 0.25 eV which equals the band bending occurring in the PTCDA substrate. The small shifts of the Zn(2p) line follow the shifts of the O(1s) line. Therefore, we conclude that there is no band bending present in the overlayer and the total band bending across the interface is

$$V_b(\text{tot}) = V_b(\text{PTCDA}) = 0.25\ \text{eV}$$

Including V_b(tot) and the HOMO cutoff positions of the uncovered PTCDA substrate (1.68 eV) and final ZnPc layer (1.05 eV), which yields a ΔHOMO= −0.63 eV inserted into eq 2, the HOMO offset at the interface is estimated to be

$$\Delta H_{cutoff} = -0.63\ \text{eV} - 0.25\ \text{eV} = -0.88\ \text{eV}$$

Using the HCM values for PTCDA and ClInPc, the offset between the HOMO maxima was determined:

$$\Delta H_{max} = \Delta H_{cutoff} + [\text{HCM(ZnPc)} - \text{HCM(PTCDA)}]$$

$$\Delta H_{max} = -0.88\ \text{eV} + [0.43\ \text{eV} - 0.50\ \text{eV}] = -0.95\ \text{eV}$$

Inserting optical gaps (E_g(PTCDA) = 2.22 eV, E_g(ZnPc) = 2.00 eV) into eq 3, the LUMO cutoff offset amounts to

$$\Delta L_{cutoff} = -0.88\ \text{eV} - [2.00\ \text{eV} - 2.22\ \text{eV}] = -0.66\ \text{eV}$$

The interface dipole eD is estimated with eq 4 using E_{ion} of PTCDA and ZnPc, which are calculated by adding work functions and HOMO cutoff positions of clean substrate and final ZnPc layer:

$$E_{ion}(\text{PTCDA}) = 4.78\ \text{eV} + 1.68\ \text{eV} = 6.46\ \text{eV}$$

$$E_{ion}(\text{ZnPc}) = 4.28\ \text{eV} + 1.05\ \text{eV} = 5.33\ \text{eV}$$

Including these values into eq 4 together with ΔH_{cutoff} yields

$$\text{eD} = 0.88\ \text{eV} - [5.33\ \text{eV} - 6.46\ \text{eV}] = 0.25\ \text{eV}$$

Figure 9 summarizes the evaluation of the PTCDA/ZnPc heterojunction.

Conclusions

The offsets in HOMO and LUMO positions shown here for these PTCDA/phthalocyanine heterojunctions are important in

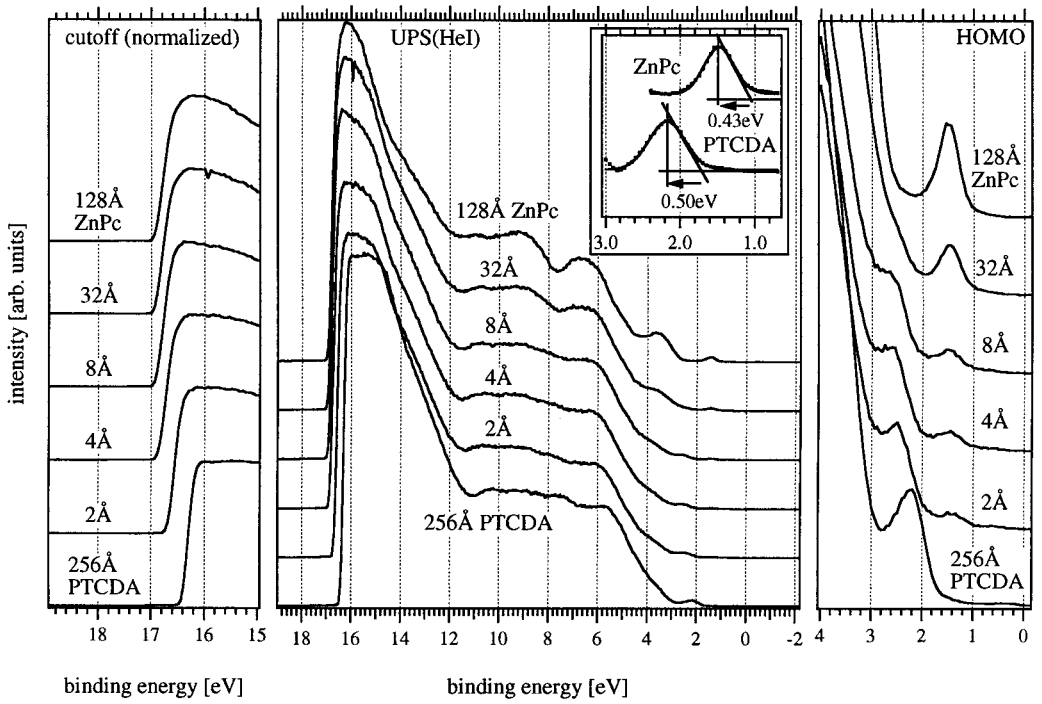

Figure 6. UPS data for the bare 256 Å PTCDA film and this same surface after each growth step of the ZnPc overlayer. In the right panel the HOMO spectra are shown magnified for more detail. The HOMO of the PTCDA layer at about 2.3 eV is successively attenuated by the increasing thickness of the ZnPc layer whose HOMO arises at about 1.4 eV. In the left panel the high binding energy cutoff is shown normalized to enhance visualization of energy shifts. The insert in the center part shows the background removed HOMO peaks of the uncovered substrate and the final ZnPc overlayer. The line fit and maxima positions which were used for the determination of the HOMO cutoff to maximum (HCM) energy for both compounds are included into the graph.

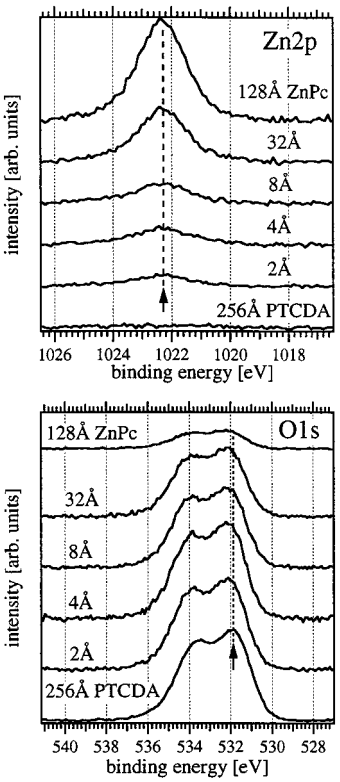

Figure 7. XPS data of the O(1s) and Zn(2p) core levels as a function of ZnPc coverage over the PTCDA layer.

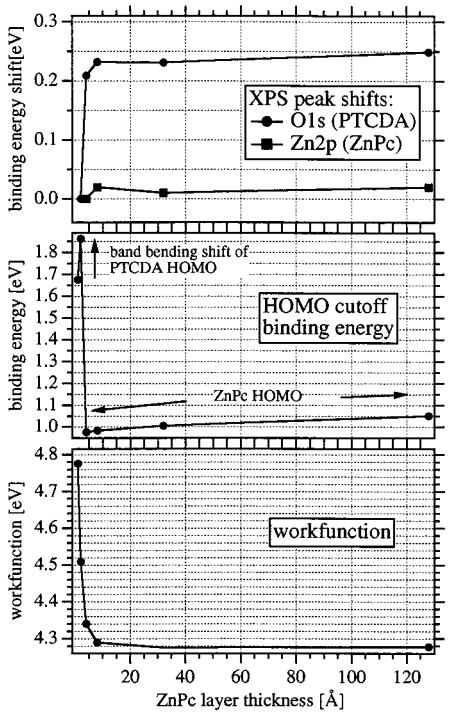

Figure 8. XPS line shifts (top), HOMO cutoff binding energy (center), and work function (bottom) as a function of the ZnPc layer thickness.

determining the rectification properties of such thin films, and in the influence that such heterojunctions play in photovoltage formation and exciton dissociation, all occurring within a few molecular layers of the heterojunction interface.[1,3,5] At the same time it has been suggested that these same HOMO/LUMO offsets at similar organic heterojunctions help to control the efficiencies of organic electroluminescent devices.[25] The approach to measuring these offsets, presented here, differs somewhat from previous approaches[6] in that both UPS and XPS measurements are necessary to fully evaluate the charge redistribution which occurs during formation of organic/organic′ heterojunctions. Using only UPS of extremely thin films on a

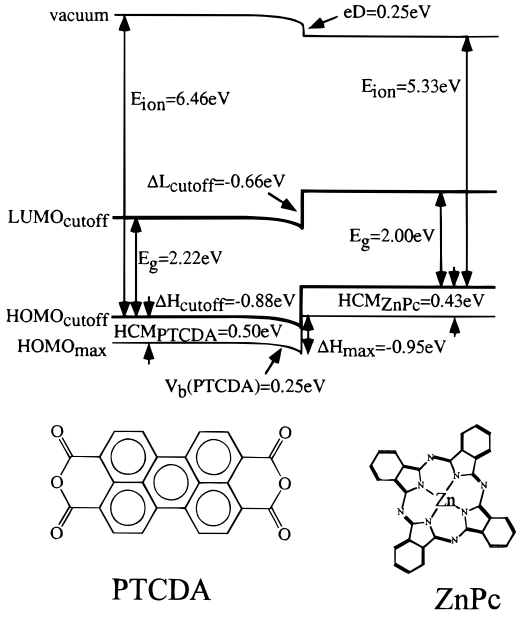

Figure 9. Summary of the evaluation of the HOMO/LUMO alignment at the PTCDA/ZnPc heterointerface. The HOMO offset between PTCDA and ZnPc was determined to be −0.88 eV (cutoff) and −0.95 eV (maxima). From known values for the HOMO−LUMO gaps the cutoff offset of the LUMO was determined to be −0.66 eV. An interface dipole of 0.25 eV is present at the interface which reduces the magnitude of the offsets between HOMOs and LUMOs.

variety of conductive substrates can provide a reasonable picture of the offsets in HOMO energies between two different organic materials, but may be altered from the characterization presented here due to the differing extent of interaction with the substrate, which may take equivalent film thicknesses of tens of nanometers to dissipate. As shown previously for a variety of inorganic semiconductor heterojunctions, measuring the absolute binding energies, in both XPS and UPS experiments, accompanied by careful measurement of the high binding energy cutoff energies and the onsets for photoionization, provides a more complete characterization of these offsets and charge redistribution process.[7−11] In theory, only UPS spectra would be necessary for these experiments; however, the shifts in core level energies which accompany heterojunction formation are difficult to resolve in UPS, whereas in XPS these core level shifts are straightforward to evaluate.

These studies suggest that there is a large interface dipole (leading to an energy offset of 0.25 vs 0.05 eV) and a larger ΔH_{max} (−0.95 vs −0.86 eV) for the ZnPc/PTCDA versus the ClInPc interface. This is consistent with expectations from gas phase photoelectron spectroscopic[26] and from previous electrochemical studies which have shown that the first oxidation potential, in nonaqueous solvents for ClInPc is ca. 0.25 V more positive than for ZnPc (+0.8 to 0.9 V vs SCE for ClInPc; +0.67 to +0.78 V vs SCE for ZnPc).[27] The exact position of the LUMOs for both the Pcs and PTCDA is more problematic to determine. Recent inverse photoionization spectroscopy measurements for PTCDA films provide an estimate of the LUMO position for this material, and an estimate of its "band gap energy" which is relatively close to the optical gap determined from the absorbance spectra of comparable thin films and which is used in our studies here.[28,29] Similar studies have not yet been conducted on the Pc films, so we are left to estimate the LUMO positions from a combination of optical and electrochemical measurements. Previous electrochemical studies suggest that the first reduction potential for ClInPc will be 0.2−0.3 V more positive than for ZnPc, as was the case for their oxidation processes (−0.7 V vs SCE for ClInPc; −0.89 to −0.94 V vs SCE for ZnPc).[27] The difference between first oxidation and first reduction potentials for these molecules, from several studies, is between 1.6 and 1.7 V, which provides a lower limit estimate to the "band gap" for these materials at low coverages, on the PTCDA surface.

Previous electrochemical studies of PTCDA in DMF,[30] and recent studies of poly(ethylene oxide)-modified bisimides of PTCDA (PTCDI−PEO), which increases the solution solubility of these materials,[31] show that the first reduction potential of the perylenetetracarboxylicdianhydride core is −0.5 to −0.6 V vs SCE, in either acetonitrile or DMF solutions, i.e., 0.35−0.41 V more positive of the first reduction potential of ZnPc and ca. 0.20 V more positive of the first reduction potential of ClInPc. On the basis of only these estimates of relative electron affinities we would expect PTCDA to act as a better electron acceptor toward ZnPc vs ClInPc, which may help to explain the differences seen in the interface dipole between the two heterojunctions reported here.

The changes in both ground state, excited state, and redox potentials which arise in the aggregated state of these materials are well documented,[14,21] and will undoubtedly alter this energetic picture somewhat. The optical band gaps shown in Figures 5 and 9, used to estimate LUMO positions for ZnPc and ClInPc layers, are based upon absorbance spectra of thin films of these materials. For the ClInPc system, deposited on well-ordered layers of PTCDA, our previous work suggests that the optical gap measured from the absorbance maximum (ca. 760 nm) will be the same as that observed for the growth of ClInPc on ordered substrates such as SnS_2, where layered growth has been clearly achieved.[14b] For the ZnPc system, layered growth may not be its preferred growth mode on PTCDA thin films, since its stable bulk structure does not possess layer planes, and its islandlike growth has been documented on a variety of substrates.[13a] Ordered thin films, however, have been created in a related heterojunction, the CuPc/PTCDA system, over film thicknesses comparable to those discussed here.[14c] The thickness of the ZnPc deposit in Figures 6−8, nevertheless, is likely to be less reliably known than for the ClInPc system, and the full development of the charge redistribution seen at this interface probably occurs at much smaller distance scale than indicated in Figures 8 and 9, for individual, nanometer-scale, ZnPc/PTCDA heterojunctions. The initial charge transfer events, however, seen here in the development of the interface dipole, are likely to be representative of all such heterojunctions based upon Pcs with comparable electron affinities and ionization potentials.

Extension of these studies is underway to a broader range of organic dyes, especially those with the capability of forming molecularly sharp interfaces and exhibiting layered growth. We are also studying the exciton quenching properties of such heterojunctions, inasmuch as this directly pertains to their ability to generate mobile charge carriers and affects their performance in photovoltaic and electrophotographic devices.[1,2,5]

Acknowledgment. This research was supported in part by the National Science Foundation (Chemistry, N.R.A.), the ONR-MURI Center for Advanced Multifunctional Polymers and Molecular Assemblies (CAMP, N.R.A.) by the Materials Characterization Program-State of Arizona, and by the Deutsches Forschungsgemeinschalt (R.S.)

References and Notes

(1) (a) Tang, C. W. *Appl. Phys. Lett.* **1986,** *48*, 183. (b) Gregg, B. A.; *Chem. Phys. Lett.* **1996**, *258*, 376. (c) Danziger, J.; Dodelet, J. P.; Armstrong,

N. R. *Chem. Mater*. **1991**, *3*, 821. (d) Schlettwein, D.; Jäger, N. I.; Wöhrle, D. *Ber. Bunsen-Ges. Phys. Chem.* **1991**, *95*, 1526. (e) Yanagi, J.; Tsukatani, K.; Yamaguchi, K.; Ashida, M.; Schlettwein, D.; Wöhrle, D. *J. Electrochem. Soc.* **1993**, *140*, 1942. (f) Wöhrle, D.; Kreienhoop, L.; Schlettwein, D. In *Phthalocyanines, Properties and Applications*; Lever, A. B. P., Leznoff, C., Eds.; VCH Publications: New York, 1996; Vol. 4, pp 219−284, and references therein. (g) Danziger, J.; Dodelet, J. P.; Lee, P.; Nebesny, K. W.; Armstrong, N. R. *Chem. Mater.* **1991**, *3*, 812.

(2) (a) Ostrick, J. R.; Dodabalapur, A.; Torsi, L.; Lovinger, A. J.; Kwock, E. W.; Miller, T. M.; Galvin, M.; Berggren, M.; Katz, H. E. *J. Appl. Phys.* **1997**, *81*, 6804. (b) Gregg, B. A. Sprague, J., Peterson, M. W.; *J. Phys. Chem.*, **1997**, *101*, 5362. (c) Adams, D. M.; Kerimo, J.; Olsen, E. J. C.; Zaban, A.; Gregg, B. A.; Barbara, P. F. *J. Am. Chem. Soc.*, **1997**, *119*, 10608. (d) Rajagopal, A.; Kahn, A. *Adv. Mater* **1998**, *10*, 140. (e) Haskal, E. I.; So, F. F.; Burrows, P. E.; Forrest, S. R. *Appl. Phys. Lett.* **1992**, *60*, 3232. (f) So, F. F.; Forrest, S. R. *Phys. Rev. Lett.* **1991**, *66*, 2649. (g) So, F. F.; Forrest, S. R.; Shi, Y. Q.; Steier, W. H. *Appl. Phys. Lett.* **1992**, *56*, 674. (h) Forrest, S. R.; Leu, L.-Y.; So, F. F.; Yoon, W. Y. *J. Appl. Phys*. **1989**, *66*, 5908.

(3) (a) Horowitz, G.; Kouki, F.; Spearman, P.; Fichou, D.; Nogues, C.; Pan, X.; Garnier, F. *Adv. Mater*. **1996**, *8*, 242. (b) Katz, H. E. *J. Mater. Chem*. **1997**, *7*, 369. (c) Bao, Z.; Lovinger, A. J.; Dodabalapur, A. *Appl. Phys. Lett* **1996**, *69*, 3066. (d) Bao, Z.; Lovinger, A. J.; Dodabalapur, A. *Adv. Mater*. **1997**, *9*, 42. (e) Lovinger, A. J.; Rothberg, L. J. *J. Mater. Res.* **1996**, *11*, 1581.

(4) (a) Ioannidis, A.; Dodelet, J.-P. *J. Phys. Chem*. **1997**, *101*, 5100. (b) Schlettwein, D.; Jaeger, N. I.; Wörhle, D. *Ber. Bunsen-Ges. Phys. Chem.* **1991**, *95*, 1526.

(5) (a) Schlettwein, D.; Armstrong, N. R. *J. Phys. Chem.* **1994**, *98*, 11771. (b) Schlettwein, D.; Armstrong, N. R.; Lee, P. A.; Nebesny, K. W. *Mol. Cryst. Liq. Cryst.* **1994**, *253*, 161. (c) Hillier, S.; Schlettwein, D.; Armstrong, N. R.; Wörhle, D. *J. Mater. Chem.* **1998**, *8*, 945. (d) Schmidt, A.; Anderson, M. L.; Dunphy, D.; Wehrmeister, Th.; Müllen, K. *Adv. Mater*. **1995**, *7*, 722. (e) Schmidt, A.; Anderson, M. L.; Armstrong, N. R. *J. Appl. Phys.* **1995**, *78*, 5619. (f) Hirose, Y.; Wu, C. I.; Aristrov, V.; Soukiassan, P.; Kahn, A. *Appl. Surf. Sci.* **1997**, *113/114*, 291. (g) Seki, K.; Ito, E.; Ishii, H. *Synth. Met.* **1997**, *91*, 137. (h) Sugiyama, K.; Yoshimura, D.; Ito, E.; Miyazaki, T.; Hamatani, Y.; Kawamoto, I.; Ishii, H.; Ouchi, Y.; Seki, K. *Synth. Met.* **1997**, *86*, 2425.

(6) (a) Popovic, Z. D.; Hor, A. M.; Loutfy, R. O. *Chem. Phys.* **1988**, *127*, 4. (b) Popovic, Z. D.; Menzel, E. R. *J. Chem Phys.* **1979**, *71*, 5090. (c) Popovic, Z. D. *J. Chem. Phys.*, **1982**, *77*, 498. (d) Popovic, Z. D. *J. Chem. Phys*. **1983**, *78*, 1552. (e) Popovic, Z. D.; Loutfy, R. O.; Hor, A. M. *Can. J. Chem.* **1985**, *63*, 134.

(7) Schlaf, R.; Lang, O.; Pettenkofer, C.; Jaegermann, W.; Armstrong, N. R. *J. Vac. Sci. Technol.* **1997**, *A15*, 1365−1370.

(8) (a) Schlaf, R.; Louder, D.; Lang, O.; Pettenkofer, C.; Jaegermann, W., Nebesny, K. W.; Lee, P. A.; Parkinson, B. A.; Armstrong, N. R. *J. Vac. Sci. Technol.* **1995**, *13*, 1761. (b) Lang, O.; Klein, A., Pettenkofer, C.; Jaegermann, W.; Chevy, A. *J. Appl. Phys.* **1996**, *80*, 3817. (c) Klein, A.; Loher, T.; Tomm, Y.; Pettenkofer, C.; Jaegermann, W. *Appl. Phys. Lett.* **1997**, *70*, 1299.

(9) Horn, K. *Appl. Phys.* **1990**, *A51*, 289.

(10) Waldrop, J. R.; Grant, R. W. *Phys. Rev. Lett.* **1979**, *43*, 1686−1689.

(11) (a) Schlaf, R.; Parkinson, B. A.; Lee, P. A.;. Nebesny, K. W.; Armstrong, N. R. *Appl. Phys. Lett*. **1998**, *73*, 1026. (b) Shimada, T.; Hamaguchi, K.; Koma, A.; Ohuchi, F. S. *Appl. Phys. Lett.* **1998**, *72*, 1869.

(12) (a) Seah, M. P. In *Practical Surface Analysis by Auger and X-ray Photoelectron Spectroscopy*; Briggs, D., Seah, M. P., Eds.; John Wiley and Sons: New York, 1983; pp 181−216 and references therein.

(13) (a) Schmidt, A.; Chau, L.-K.; Back, A.; Armstrong, N. R. In *Phthalocyanines*; Lever, A. B. P., Leznoff, C., Eds.; VCH: New York, 1996; Vol. 4; pp 307−341. (b) Arbour, C.; Chau, L.-K.; Collins, G. E.; Nebesny, K. W.; Lee, P. A.; England, C. D.; Parkinson, B. A. *J. Phys. Chem.* **1993**, *97*, 2690.

(14) (a) Schlettwein, D.; Back, A.; Schilling, B.; Fritz, T.; Armstrong, N. R. *Chem. Mater*. **1998**, *10*, 601. (b) Anderson, M. L.; Collins, G. E.; Williams, V. S.; England, C. D.; Chau, L.-K.; Schuerlein, T. J.; Lee, P. A.; Nebesny, K. W.; Armstrong, N. R. *Surf. Sci.* **1994**, *551*, 307−309. (c) Schuerlein, T. J.; Armstrong, N. R. *J. Vac. Sci. Technol. A* **1994**, *4*, 12.

(15) Schlaf, R.; Armstrong, N. R.; Parkinson, B. A.; Pettenkofer, C.; Jaegermann, W. *Surf. Sci*. **1997**, *385*, 1−14.

(16) Jaegermann, W.; Tributsch, H. *Prog. Surf. Sci* **1988**, *29*, 1−167.

(17) Jaegermann, W. In *Photoelectrochemistry and Photovoltaics of Layered Seminconductors, Physics and Chemistry of Materials with Low-Dimensional Structures*; Aruchamy, A., Ed.; Kluwer Academic Press: Boston, 1992; Vol. 14.

(18) Schuerlein, T. J.; Schmidt, A.; Lee, P. A.; Nebesny, K. W.; Armstrong, N. R. *Jpn. J. Appl. Phys.* **1995**, *34*, 3837.

(19) Ludwig, C.; Gompf, B.; Petersen, J.; Strohmaier, R.; Eisenmenger, W. *Z. Phys.* **1994**, *B93*, 365−373.

(20) Kendrick, C.; Kahn, A.; Forrest, S. R. *Appl. Surf. Sci.* **1996**, *104/105*, 586.

(21) Chau, L.-K.; England, C. D.; Chen, S.; Armstrong, N. R. *J. Phys. Chem.* **1993**, *97*, 2699.

(22) Ertl, G.; Küppers, J. *Low Energy Electrons and Surface Chemistry*, VCH: Weinheim, Germany, 1985.

(23) Anderson, R. L. *Solid State Electronics* **1962**, *5*, 341.

(24) Schmidt, A.; Schuerlein, T. J.; Collins, G. E.; Armstrong, N. R. *J. Phys. Chem.* **1995**, *99*, 11770.

(25) (a) Tang, C. W.; VanSlyke, S. A. *Appl. Phys. Lett.* **1987**, *51*, 913. VanSlyke, S. A.; Chen, C. H.; Tang, C. W. *Appl. Phys. Lett.* **1996**, *69*, 2160.

(26) Lee, P. A.; Armstrong, N. R. Work in progress.

(27) Lever, A. P. B.; Milaeva, E. R.; Speier, G. *Phthalocyanines: Properties and Applications*; Lever, A. P. B., Leznoff, C. C., Eds.; VCH Publications: New York, 1991; pp 9−18, and references therein.

(28) Rajagopal, A.; Kahn, A. *Adv. Mater*. **1998**, *10*, 140.

(29) Rajagopal, A.; Wu, C. I.; Kahn, A. *J. Appl. Phys*. **1998**, *83*, 2649.

(30) DeLuca, C.; Giomini, C.; Rampazzo, L. *J. Electroanal. Chem.* **1987**, *238*, 215.

(31) Nablo, B.; Belsher, A.; Armstrong, N. R. Manuscript in preparation.